Journal of the Meteorological Society of Japan, Vol. 85B, pp. 385–403, 2007

Role of Ocean in Global Warming

Syukuro MANABE

Program in Atmospheric and Oceanic Sciences, Princeton University, Princeton, New Jersey, USA

and

Ronald J. STOUFFER

National Oceanic and Atmospheric Administration / Geophysical Fluid Dynamics Laboratory, Princeton, New Jersey, USA

(Manuscript received 18 October 2006, in final form 2 February 2007)

Abstract

Based upon the results obtained from coupled ocean-atmosphere models of various complexities, this review explores the role of ocean in global warming. It shows that ocean can play a major role in delaying global warming and shaping its geographical distribution. It is very encouraging that many features of simulated change of the climate system have begun to agree with observation. However, it has been difficult to confirm the apparent agreement because the density and frequency of the observation are insufficient in many oceanic region of the world, in particular, in the Circumpolar Ocean of the Southern Hemisphere. It is therefore essential to intensify our effort to monitor not only at the surface but also in the subsurface layers of oceans.

1. Early studies

When the concentration of greenhouse gas increases, the outgoing flux of long wave radiation at the top of the atmosphere decreases, and is responsible for the warming of the troposphere. On the other hand, the increase in the concentration of greenhouse gas results in the increase in the downward flux of long wave radiation at the Earth's surface, providing additional heat to the Earth's surface. Over continental surfaces, much of the additional heat is returned back to the troposphere through evaporation, sensible heat flux, and radiative heat transfer. Over ocean, however, a substantial fraction of the additional heat is transferred downward into the ocean through convection, small-scale eddies, and large-scale circulation, helping to reduce the warming at oceanic surface. The reduction in the warming at oceanic surface accompanies the reduction of similar magnitude over continent because of the atmospheric heat exchange between oceanic and continental regions. This is why the rate of increase in surface temperature is delayed not only over oceans but also over continents.

Using a globally averaged, energy balance model of the atmosphere, Schneider and Mass (1975) investigated the time dependent response of surface temperature to thermal forcing such as the reflection of solar radiation by volcanic sulfate aerosols. In response to an idealized switch-on thermal forcing (defined as Q, where $Q = 0$ for times, $t < 0$, and $Q = Q_0$ for $t \geq 0$), the surface temperature changes according to the following equation.

Corresponding Author: Syukuro Manabe, Program in Atmospheric and Oceanic Sciences, Princeton University, Sayre Hall, Forrestal Campus, PO Box CN710, Princeton, NJ 08544-0710, USA.
E-mail: manabe@splash.princeton.edu
© 2007, Meteorological Society of Japan

$$C\partial T_S/\partial t = Q - \lambda T_S, \quad (1)$$

where C is the heat capacity of the system, and t is time. T_S is the deviation of surface temperature from the initial value, λ is the so-called feedback parameter, which represents the rate of the damping of surface temperature anomaly due to the outgoing radiation from the top of the atmosphere. The solution of Eq. (1) is given by

$$T_S = (T_S)_{t=\infty}(1 - \exp(-t/\tau)), \quad (2)$$

where $(T_S)_{t=\infty}$ represents the so-called, equilibrium response of surface temperature, i.e., the response to be realized, given sufficient length of time. It is given by

$$(T_S)_{t=\infty} = Q_0/\lambda, \quad (3)$$

In Eq. (2), τ represents the so-called e-folding time of the response, when $1/e$ of the total response remains to be realized. It represents the delay of the response due to the thermal inertia of the system (C) and is given by

$$\tau = C/\lambda, \quad (4)$$

As Eq. (4) shows, the delay of the response is inversely proportional to the feedback parameter that determines the sensitivity of climate, and is proportional to the effective heat capacity of the system, implying the larger is the thermal inertia of the system, the longer is the delay in surface warming.

In response to the increase in greenhouse gas in the atmosphere, the positive temperature anomaly initially appears in the well-mixed surface layer of ocean called the "mixed layer". Gradually, the anomaly spreads from the mixed layer to the deeper layers of ocean, thereby increasing the effective heat capacity of oceans. The increase of effective heat capacity, in turn, results in the reduction of the rate of the increase in surface temperature, reducing and delaying the warming as shown by Hoffert et al. (1980), and Hansen et al. (1984).

Using one-dimensional energy balance model of the atmosphere combined with the mixed layer model of ocean, Schneider and Thompson (1981) evaluated the delay in the response of sea surface temperature to gradual increase in the atmospheric carbon dioxide. Their study shows that time-dependent response of zonal mean surface temperature differs significantly from its equilibrium response particularly in those latitude belts, where the fraction of ocean-covered area is relatively large. Based upon the study, they conjectured that the response of surface temperature in the Southern Hemisphere should be delayed as compared to that in the Northern Hemisphere because of the inter-hemispheric difference in the fraction of the area covered by oceans.

Using a coupled ocean-atmosphere model, in which a general circulation model of the atmosphere is combined with that of ocean, Bryan et al. (1988) investigated the role of ocean in shaping the CO_2-induced warming of the Earth's surface. The coupled model has so-called sector domain bounded by two meridians that are 180° apart. Cyclic continuity is maintained in the model atmosphere between the two meridians. The land-ocean fraction at each latitude belt is realistic with a zonally connected ocean at the latitude of the Drake Passage. In their numerical experiment, the coupled model is subjected to a switch-on thermal forcing, in which the atmospheric CO_2 concentration doubles abruptly and remains unchanged thereafter. They found that the increase in surface temperature is very small in the Circumpolar Ocean of the Southern Hemisphere in sharp contrast to high latitudes of the Northern Hemisphere, where the increase is relatively large. This result is in qualitative agreement with the result obtained earlier by Schneider and Thompson (1981). However, the detailed analysis of the numerical experiment reveals that the absence of substantial surface warming in the Circumpolar Ocean is attributable not only to the large fraction of the area covered by the ocean but also to the deep penetration of positive temperature anomaly into the ocean.

In the same year, Hansen et al. (1988) at Goddard Institute for Space Studies (GISS) of NASA published a landmark study of the time-dependent response of climate. Using a global coupled ocean-atmosphere model with realistic geography, they estimated the geographical distribution of climate change in response to the best-guess estimate of radiative forcing, which includes not only the increase in carbon dioxide but also the change in other trace constituents such as methane, nitrous oxide, CFC, and sulfate aerosols of volcanic origin. Encour-

aged by the success in approximately reproducing the increase in global mean surface temperature during the latter half of 20th century, they projected future climate change. Hansen presented the results of this study at the public hearing organized by a committee of US Senate. He conjectured that global warming had already begun and is likely to continue. His testimony had a far-reaching impact upon the public awareness of this critical issue of the global environment.

In the oceanic component of the coupled model, which was used by Hansen et al. (1984), the downward penetration of heat below the mixed layer was expressed as vertical diffusion. In the actual ocean, however, heat is transported downward not only by small scale eddies and convection but also by three-dimensional, large-scale circulation. This is why it is not appropriate to express oceanic heat transport as vertical diffusion. Instead, it is desirable to explicitly incorporate the heat transport by general circulation not only in the atmosphere but also in oceans. Although such a model was already used by Bryan et al. (1982, 1988) for the study of global warming, the model had a limited computational domain and a highly idealized geography.

Washington and Meehl (1989) and Stouffer et al. (1989) were the first to use a general circulation model of the coupled atmosphere-ocean-land system with the global domain and realistic geography. The latter study was followed by the two companion studies conducted by Manabe et al. (1991, 1992). Based upon detailed analysis of a set of numerical experiments conducted at GFDL, these studies explore the physical processes that control the time-dependent response of climate to CO_2 forcing. In the following section, we shall describe some of the highlights of the results obtained from these studies.

2. Global warming experiment

2.1 Model structure

The coupled model used for these studies is described by Manabe et al. (1991). It consists of general circulation models (GCMs) of the atmosphere and oceans, and a simple model of heat and water budget at continental surface. In contrast to the early versions of the coupled model with limited computational domains and

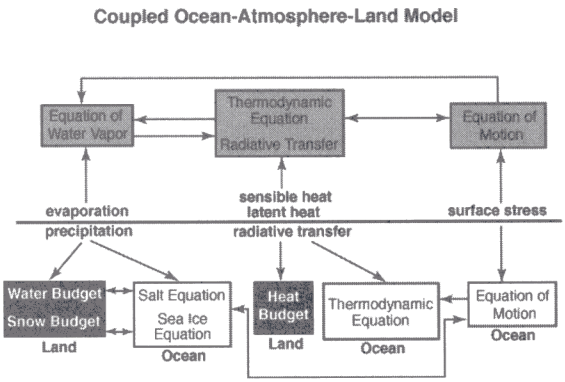

Fig. 1. Box diagram that depicts the structure of the coupled ocean-atmosphere model.

idealized geographies (Manabe and Bryan 1969; Bryan et al. 1988), it has a global computational domain with realistic geography.

The atmospheric GCM has prognostic system of wind, temperature, and humidity, which uses the equation of motion, thermodynamical equation, and continuity equation of water vapor, respectively (Fig. 1). The absorption of solar radiation and the absorption and emission of long wave radiation are computed using radiative transfer equations. The distribution of cloud cover is determined from the distribution of relative humidity. The atmospheric model is coupled with a simple model of heat and water budget at continental surface (Manabe 1969).

The oceanic GCM predicts ocean currents, temperature, and salinity, using the equation of motion, thermodynamical equation, and prognostic equation of salinity. It is coupled with a simple model of sea ice (Bryan 1969). The atmospheric and oceanic GCMs interact with each other continuously through the exchanges of heat, water and momentum as illustrated in Fig. 1.

Because of the limited capability of computers available around the late 1980's, the computational resolution of the model is substantially lower than the state-of-art coupled models in use today. The atmospheric GCM had nine vertical finite difference levels. The horizontal distributions of predicted variables are represented by spherical harmonics (15 associated Legendre functions for each of Fourier components) and grid point values. The oceanic GCM

has a regular grid system with 4.5° × 3.75° (latitude × longitude) spacing and 12 vertical finite difference levels (Bryan and Lewis 1979).

2.2 Numerical experiments

To study the response of the coupled model to a gradual increase of atmospheric carbon dioxide, two 100-yr integrations of the model were performed. Starting from an initial condition in a quasi-equilibrium state, the control experiment used the normal concentration of atmospheric carbon dioxide (i.e., 300 ppm by volume), which does not change with time. In the other experiment, the CO_2 concentration was increased by 1% per year (compounded), doubling its value by year 70. The rate of 1% per year was chosen because the total CO_2-equivalent amount of various greenhouse gases other than water vapor was increasing at approximately this rate around 1990, when this experiment was performed. The time-dependent response of the coupled model to increasing carbon dioxide was determined from the difference between the two time integrations.

2.3 Time-dependent response

In response to the gradual increase in carbon dioxide, the globally averaged surface air temperature increases monotonically at the rate of ~3.5°C per century as indicated by solid line in Fig. 2. By the ~70th year of the experiment, when the atmospheric CO_2 concentration doubles, the global mean surface temperature increases by about 2.4°C. (In the 2001 IPCC Working Group I report, this value is defined as the transient climate response, Cubasch et al. 2001).

Figure 3 illustrates the pattern of surface air temperature change that occurs by the ~70th year of the experiment. As this figure shows, the surface warming is usually larger over continents than over the oceans particularly over Eurasian and North American continents. As shown by Manabe et al. (1992), the land-sea contrast in warming appears during both winter and summer. In winter, it is attributable mainly to the positive feedback effect of snow cover, which reflects a major fraction of solar radiation that reaches continental surface. As continental surface warms due to the increase in the downward flux of long wave radiation, snow cover retreats poleward, and exposes

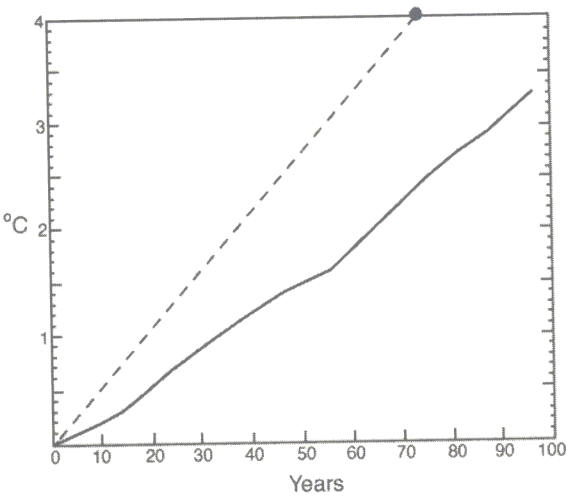

Fig. 2. The solid line shows the time-dependent response of the global mean surface air temperature (°C) of the coupled atmosphere-ocean model to gradual increase of CO_2 concentration of air (at a compounded rate of 1%/year). A black dot near the top of the figure illustrates the equilibrium response of the global mean surface air temperature of the atmosphere-mixed layer ocean model. The dashed line, which connects the black dot and origin of the figure, approximately shows how the equilibrium response changes with time. From Manabe et al. (1991)

snow-free surface with relatively low albedo. Thus, the surface absorption of solar radiation increases, enhancing the warming over continental surface. A different mechanism is involved in enhancing the continental warming in summer. Although evaporation is responsible for removing much of heat energy over wet oceanic surface, it is not as effective in doing so over the relatively dry continental surface, where a substantial fraction of the heat energy is removed through sensible heat flux. This is why it is necessary for the surface temperature increase to be larger over continents than over oceans in summer as the downward flux of long wave radiation increases due to the increase in CO_2 concentration in air.

Figure 3 also reveals that there is large asymmetry in surface warming between the two hemispheres. In the Northern Hemisphere,

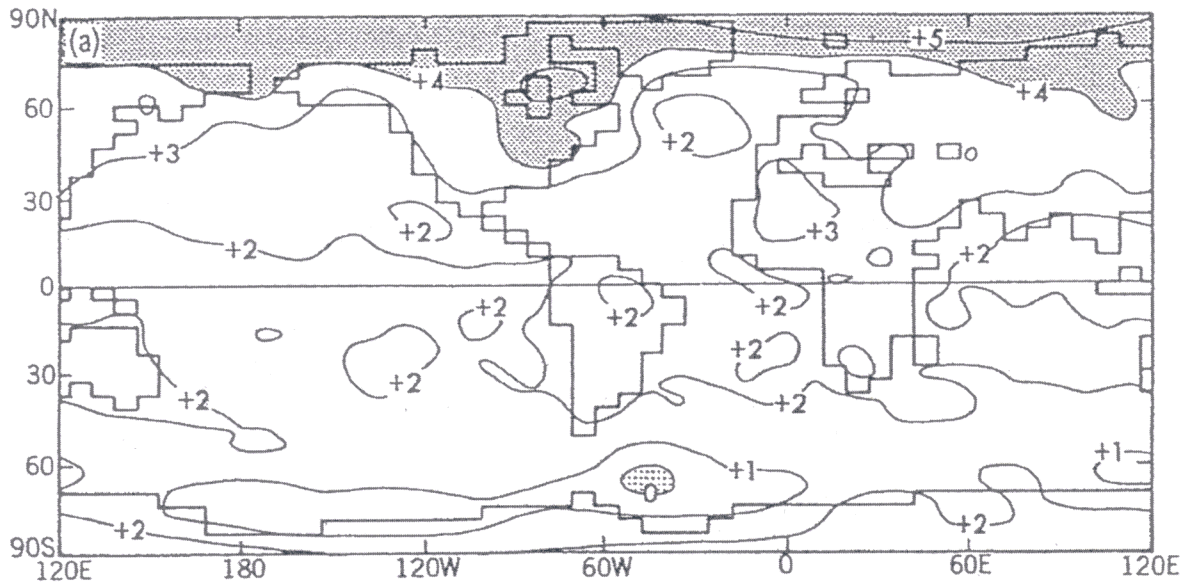

Fig. 3. Geographical distribution of the change in surface air temperature of the coupled atmosphere-ocean model, which occurs by the ~70th year (i.e., the average from the 60th to 80th year) in response to the gradual increase in CO_2 concentration of air (at a compounded rate of 1%/year). From Manabe et al. (1991)

the surface warming increases with increasing latitude, and is particularly large in Arctic Ocean. This is in sharp contrast to the Southern Hemisphere, where warming is relatively large in low latitudes and decreases with increasing latitudes. It becomes small in the Circumpolar Ocean of the Southern Hemisphere particularly in the immediate vicinity of Antarctic Continent.

The large warming in high northern latitudes is attributable mainly to the poleward retreat of sea ice and snow cover, which enhances the absorption of solar radiation by the Earth's surface. As shown in Fig. 4, which illustrates the distribution of sea ice at the beginning and the ~70th year of the experiment for two seasons of a year, sea ice thickness decreases substantially over the Arctic Ocean. The reduction in the area coverage of Arctic sea ice is pronounced in summer, when the solar radiation is large, contributing to the positive feedback effect of sea ice upon surface air temperature.

One can ask: why the polar amplification of warming does not occur in the Southern Hemisphere despite the existence of extensive sea ice, which has positive albedo feedback? As discussed in the following section, the absence of significant warming in the Circumpolar Ocean of the Southern Hemisphere is attributable mainly to the large thermal inertia of ocean, which results from very effective mixing between the surface layer and the deeper layers of ocean in this region. This is in sharp contrast to the Arctic Ocean, where very stable layer of halocline prevents the mixing between the surface layer and deeper layer of the ocean.

In view of the absence of significant surface warming, it is not surprising that the area-coverage of sea ice hardly changes in the Circumpolar Ocean (as Fig. 5 shows) despite the CO_2-doubling. It is surprising, however, that the thickness of simulated sea ice appears to be increasing with time in both Ross and Weddell Seas (Fig. 5). Because of the reduction of surface salinity due to the increased supply of ice/water from Antarctic Continent of the model, the convective mixing between the mixed layer and deeper ocean becomes less frequent, thereby allowing the sea ice thickness to increase in both Ross and Weddell Seas. The simulated increase in sea ice thickness, however, should not be taken seriously in view of highly crude treatment of land ice discharge in the model.

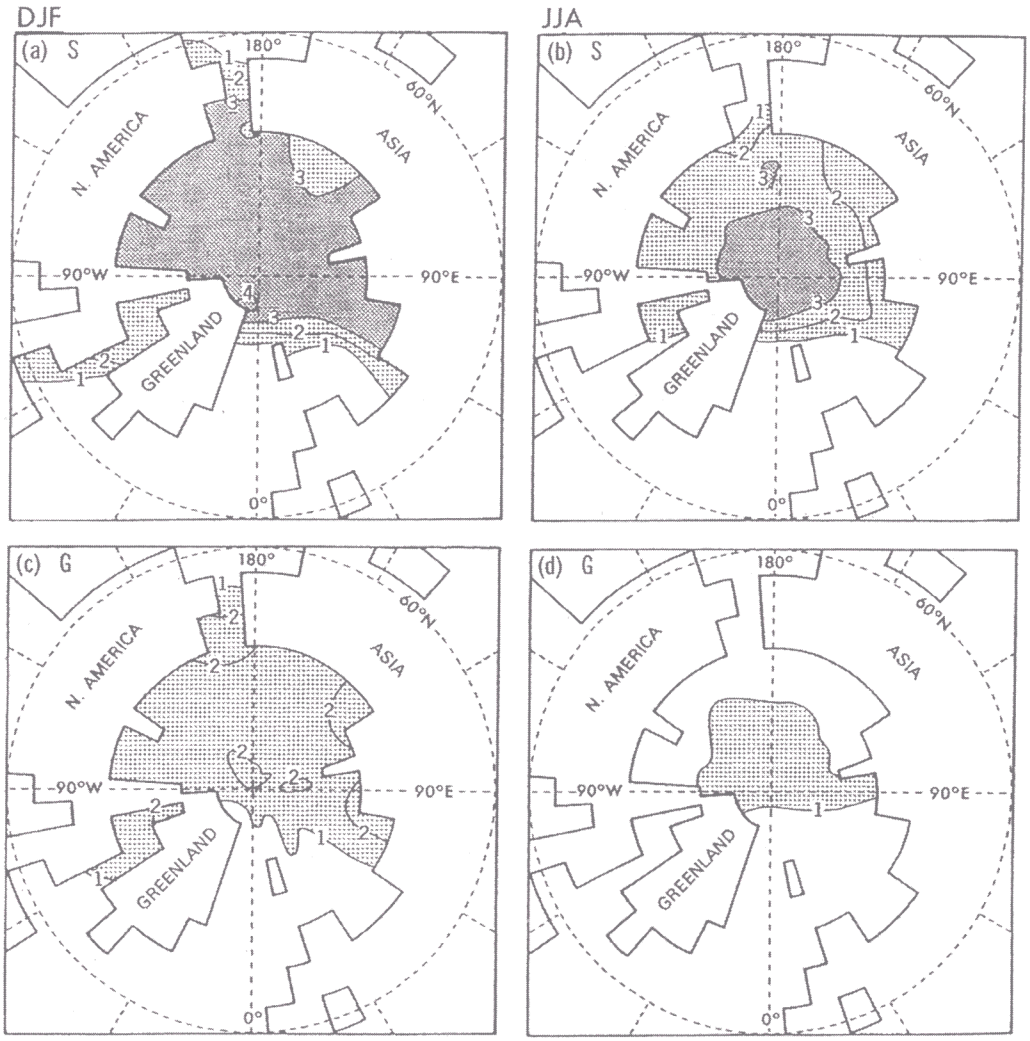

Fig. 4. Geographical distributions of the sea ice thickness over the Arctic Ocean at the beginning (i.e., 100 year average) and the ~70th year (i.e., the average from the 60th to 80th year) of the experiment for the 3-month periods of December, January and February (DJF) and June, July and August (JJA). (a) Initial thickness for DJF. (b) Initial thickness for JJA. (c) 70th year thickness for DJF. (d) 70th year thickness for JJA. Units are in meter. From Manabe et al. (1992)

2.4 Equilibrium response

In order to see how the warming of surface temperature is modified by the heat exchange between the surface layer and deeper layer of ocean, the time-dependent response of the coupled ocean-atmosphere model was compared with that of another model called "coupled mixed layer ocean-atmosphere model or slab ocean model" (Manabe and Stouffer 1979). Although the atmospheric components of the two models are identical to each other, the oceanic component of the latter model is an idealized model of the mixed layer ocean, i.e., a vertically isothermal layer of water with 50 m thickness. The effect of heat transport by ocean current is represented as heat flux at the bottom of the mixed layer ocean and remains unchanged despite global warming. As proposed by Hansen et al. (1984), the distribution of the heat flux is determined in such a way that the seasonal variation and geographical distribution of sea surface temperature and sea ice thickness are realistic in the control experiment. The structure of the atmosphere-mixed layer model

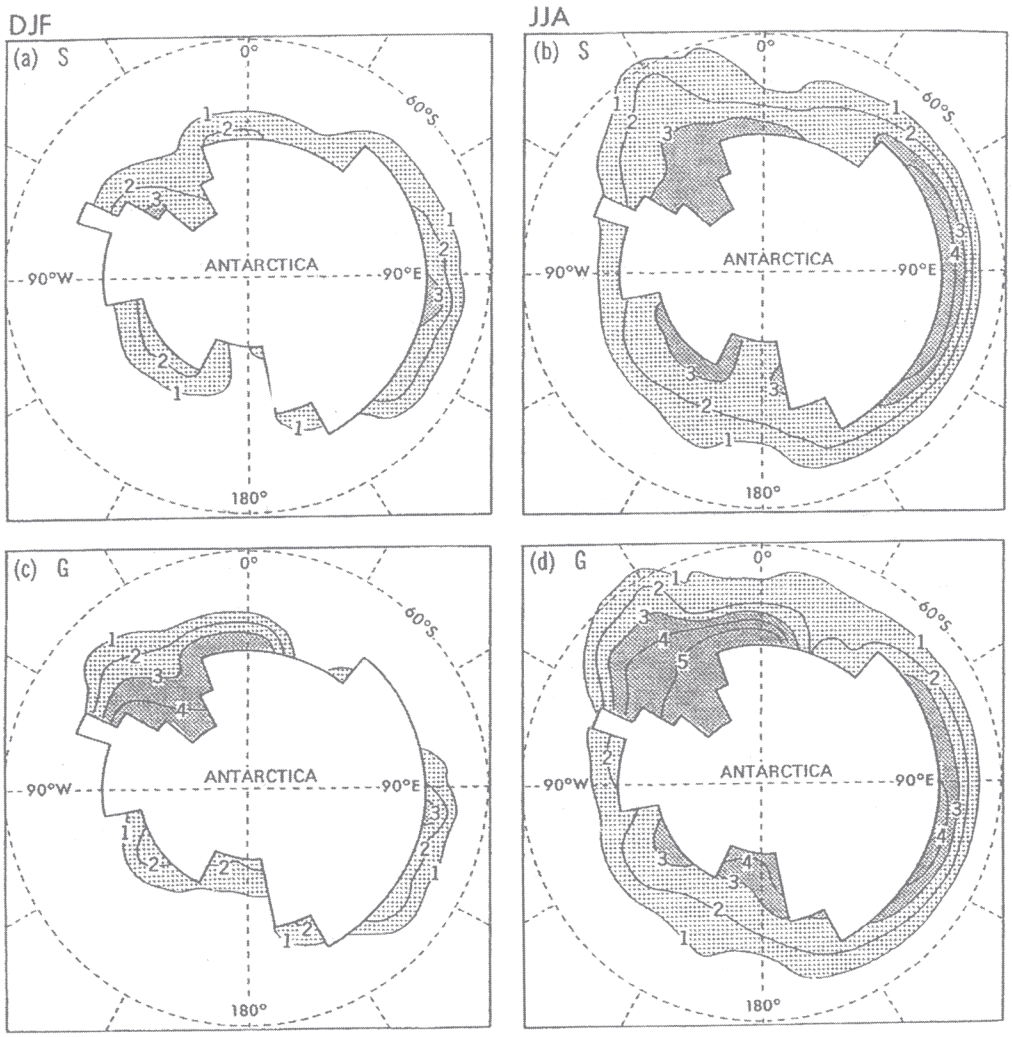

Fig. 5. Same as Fig. 4 for the Circumpolar Ocean of the Southern Hemisphere. From Manabe et al. (1992)

described here is in contrast to the coupled atmosphere-ocean GCM, in which the effect of heat exchange between the mixed layer and deeper layer of ocean gradually changes with time as temperature anomaly penetrates downward as global warming proceeds.

Because of the absence of the interaction between the mixed layer and deeper layers of ocean, the coupled atmosphere-mixed layer model rapidly approaches an equilibrium state when the radiative forcing changes. From the difference between two equilibrium states of the model with the standard and twice the standard concentration of carbon dioxide, one can estimate the equilibrium response of the model to the doubling of CO_2 concentration in the atmosphere. The difference between the equilibrium response of the mixed layer ocean-atmosphere model and the transient climate response of the coupled ocean-atmosphere model should indicate how oceans help in delaying the response of the coupled model to gradually increasing carbon dioxide in the atmosphere.

The equilibrium response of the global mean surface temperature to the CO_2-doubling is about 4°C, and is substantially larger than 2.4°C, i.e., the time-dependent response of the coupled model realized by the 70th year, when CO_2 concentration of air doubles. It is plotted as a black dot in Fig. 2 at the 70th year. In this

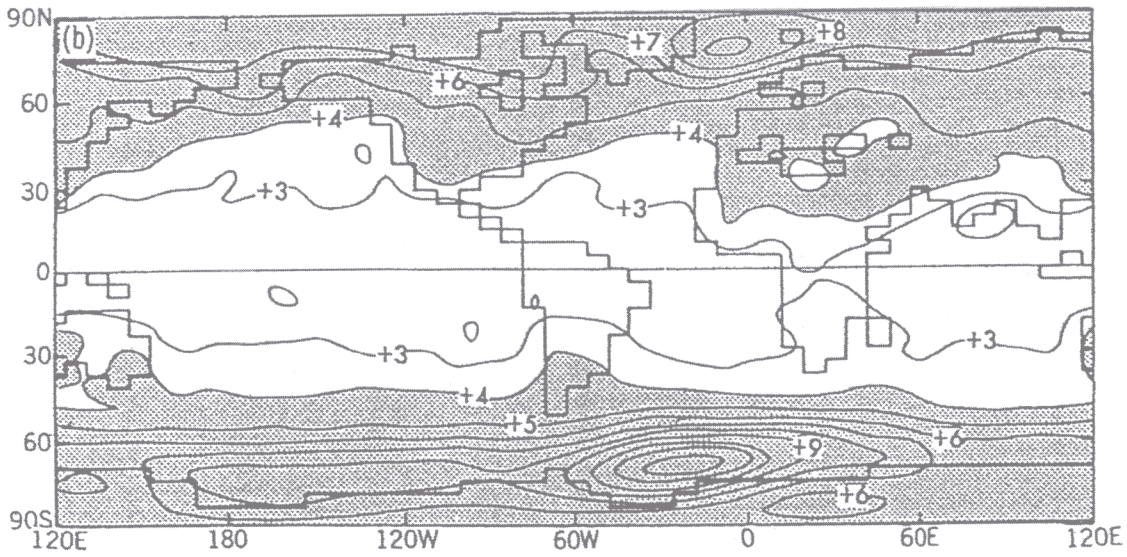

Fig. 6. Geographical distribution of the equilibrium response of surface air temperature of the coupled atmosphere-mixed layer ocean model in response to the doubling of CO_2 concentration of air. From Manabe et al. (1991)

figure, a straight dashed line is drawn between the black dot and the origin of the graph, assuming that the equilibrium response of the global mean surface temperature increases linearly as the atmospheric concentration of carbon dioxide increases exponentially with time. [This assumption is justified because the greenhouse effect of the atmosphere increases almost linearly as CO_2 concentration of air increases exponentially.] The distance between the solid and dashed lines indicates the lag of the time-dependent response behind the equilibrium response due to the thermal inertia of ocean. This figure shows that the lag is zero at the beginning of the experiment and increases gradually with time. By the 70^{th} year, when CO_2 concentration doubles, the lag is about 35 years. As global warming proceeds, the positive temperature anomaly penetrates downward into the deeper layer of ocean. Thus, the effective thermal inertia of ocean increases gradually, delaying further the time-dependent response of surface temperature (see, Hansen et al. 1984 for further discussion of this subject).

The geographical distribution of the equilibrium response of surface air temperature to the CO_2-doubling is illustrated in Fig. 6. It may be compared with the distribution of the time-dependent response of the coupled atmosphere-ocean model on the 70^{th} year, when CO_2 concentration is doubled (Fig. 3). In general, magnitude of the equilibrium response is substantially larger than that of the time-dependent response. It is particularly large not only over Arctic Ocean but also over Circumpolar Ocean of the Southern Hemisphere. This is in sharp contrast to the time-dependent response of the surface temperature of the coupled model, which is very small near the Antarctic Continent, but is large over the Arctic Ocean, exhibiting the marked asymmetry between the two hemispheres.

Figure 7 illustrates the geographical distribution of the ratio of the time-dependent response of surface air temperature (Fig. 3) to its equilibrium response (Fig. 6). Here, small ratio identifies those regions, where the time-dependent response is delayed greatly and is much smaller than the equilibrium response. As this figure indicates, the ratio is small over the wide zonal belt in the Circumpolar Ocean of the Southern Hemisphere and in a broad area of the North Atlantic Ocean located between Labrador and Scandinavian Peninsula. In these regions, the time-dependent response

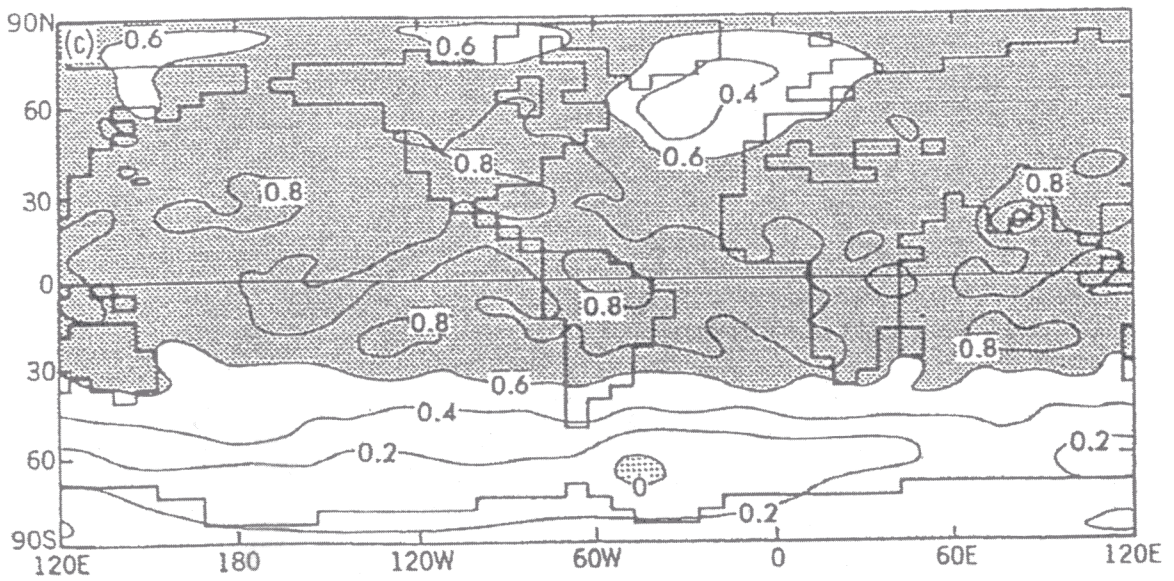

Fig. 7. Geographical distribution of the ratio of the time-dependent response of the coupled atmosphere-ocean model (Fig. 3) to equilibrium-response of the coupled atmosphere-mixed layer ocean model (Fig. 6) in response to the doubling of CO_2 concentration of air. From Manabe et al. (1991)

of surface temperature is greatly delayed due to convective and isopycnal mixing (i.e., mixing along the surface of constant density) as discussed below.

2.5 Atlantic Ocean

In the upper layers of the Atlantic Ocean, water moves northward into the vicinity of Iceland, where it is cooled by frigid air in winter off the east coast of Canada and Greenland. As the water cools, it becomes dense and sinks to the abyss near Greenland and moves southward along North and South America. At the southern tip of Africa, it joins the outer fringe of deep current that flows around the Antarctic Continent. Much of deep water thus generated eventually returns to ocean surface. The global scale, overturning circulation described above is called "The Great Ocean Conveyor" by Broecker (1991), and is illustrated schematically by Gordon (1986) as shown in Fig. 8. The total flow of water involved is about 20 million cubic meters per second (or in oceanographer's units, 20 Sverdrups). This flow is about 20 times as large as the total discharge from all rivers in the world. The conveyor transports warm upper ocean water northward to the northern North Atlantic and Nordic Seas (e.g., Norwegian and Greenland Seas), thereby helping to maintain warm climate over northern North Atlantic and its vicinity.

The coupled atmosphere-ocean model simulates the structure and intensity of the conveyor reasonably well (Manabe and Stouffer 1999). In the global warming experiment, in which CO_2 concentration of air increases gradually, the intensity of the conveyor or overturning circulation also weakens gradually. The rate of overturning is ~17 million cubic meters per second at the beginning of the experiment (Fig. 9a). By the $\sim 70^{th}$ year, when CO_2 concentration doubles, it is reduced to 12 million cubic meters per second (Fig. 9b).

As discussed by Manabe et al. (1991), for example, the gradual weakening of the conveyor is attributable mainly to the reduction of convective activity in the sinking region of the overturning circulation. As the absolute humidity of air increases due to global warming, the poleward transport of water vapor increases in the troposphere, markedly increasing the excess of precipitation over evaporation in the Arctic Ocean and the rate of river discharge from the surrounding continents. Thus, salinity

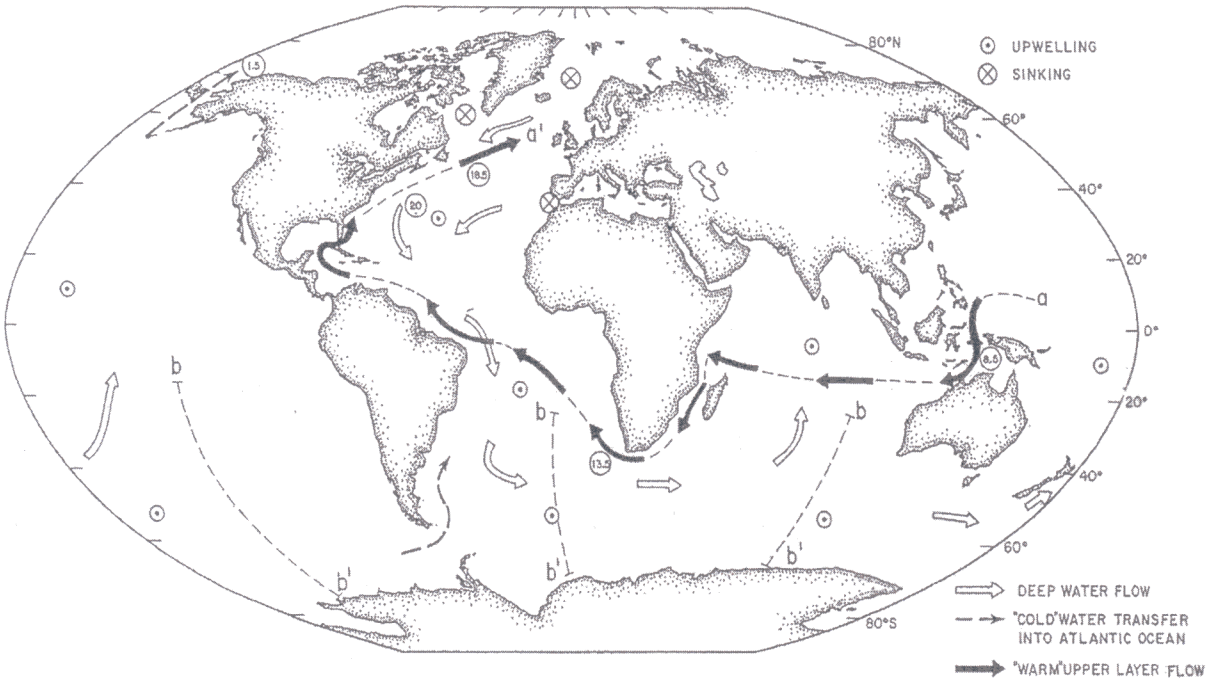

Fig. 8. Global distribution of the overturning circulation (Gordon 1986). Dark arrows indicate the direction of the upper layer flow. Blank arrows indicate the direction of deep water flow. A narrow sinking region is identified by a cross enclosed by a circle, and a broad upwelling region is indicated by a dot enclosed by a circle.

of surface water decreases in the Arctic Ocean. As the low salinity surface water flows southward along the east coast of Greenland, the density of surface water decreases in the northern North Atlantic, suppressing convection in the sinking region of the conveyor. As the convective cooling of sinking water decreases due to the weakening of convective activity, the rate of sinking decreases, weakening the conveyor. This is one of the important reasons why the simulated conveyor weakens as global warming proceeds.

The density of surface water decreases not only due to the reduction of surface salinity discussed above but also due to the increase in surface temperature. As the atmospheric concentration of carbon dioxide increases, the downward flux of long wave radiation increases as noted earlier, thereby raising sea surface temperature. Thus, the density of surface water decreases, weakening the conveyor.

As discussed above, the changes in both water and heat flux at ocean surface results in the weakening of the conveyor. The relative importance of the changes varies from model to model as shown, for example, by Dixon et al. (1999). Gregory et al. (2005) found that, in most models, the heat flux changes due to increasing atmospheric greenhouse gases weaken the conveyor by about 20%. The additional weakening is attributable more or less to the increase in the freshwater supply at oceanic surface. They found that the change in freshwater supply varies greatly from one model to another, and is partly responsible for the large inter-model difference in the magnitude of the weakening. One should note, however, that the weakening depends not only upon the magnitude of the increase in freshwater supply but also to the sensitivity of the conveyor to freshwater forcing. As noted by Stouffer et al. (2006a), there is large inter-model difference in the response of the conveyor to an identical freshwater forcing.

As the overturning circulation slows down, the northward advection of the warm upper water is reduced, moderating the warming over the extensive regions of the northern North At-

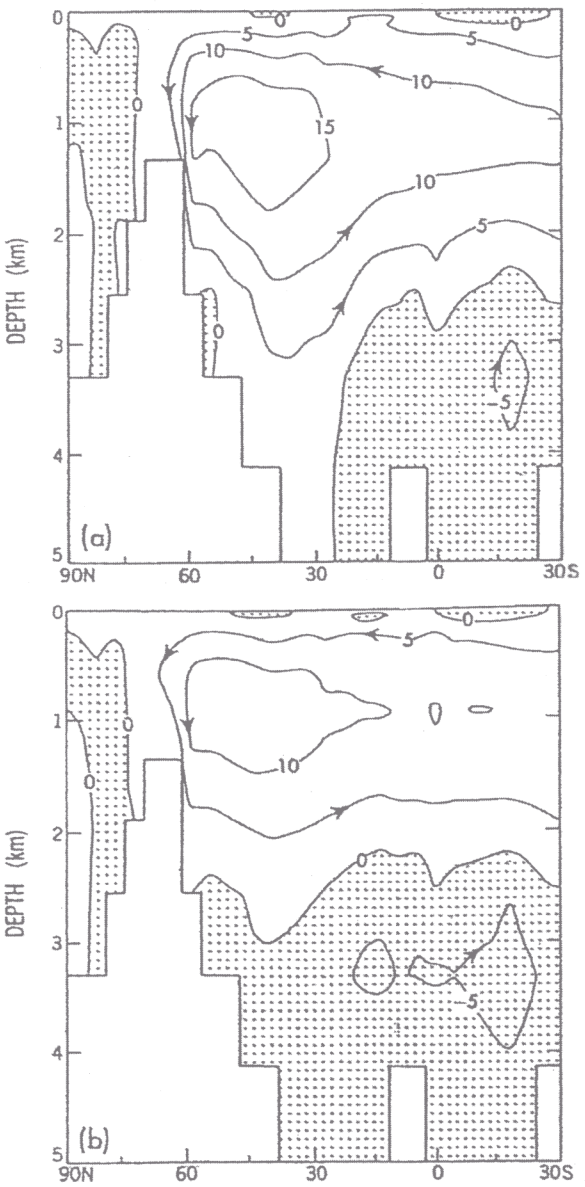

Fig. 9. Latitude-depth pattern of the streamfunction of the meridional overturning circulation in the Atlantic Ocean of the coupled model at the beginning (a) and ~70th year (i.e., the average from the 60th to 80th year) of the experiment (b). From Manabe et al. (1991)

lantic and surrounding regions. This is why surface warming is relatively small over the region that extends from the Labrador Peninsula to the West coast of Europe (Fig. 3). Because of the weakening of the conveyor, the increase in surface air temperature is relatively small not only over the narrow sinking region of the conveyor (with large vertical mixing) but also over the extensive region of the northern North Atlantic.

The global warming experiment described here was extended in time by Manabe and Stouffer (1993, 1994). Assuming the temporal variations of atmospheric carbon dioxide shown in Fig. 10a, three 500 year integrations are performed. One is the standard integration (S), in which the atmospheric CO_2 remains unchanged. In the second integration (2xC), the CO_2 concentration increases initially by 1% yr^{-1} until it doubles around 70th year and remains unchanged thereafter. In the third integration (4xC), the CO_2 concentration also increases by 1% yr^{-1} until it reaches four times the standard value at about the 140th year and remains unchanged thereafter.

Figure 10b illustrates the temporal variations of the intensity of the conveyor obtained from the three experiments. In the standard experiment (S), in which CO_2 concentration remains unchanged, the intensity of the conveyor does not change significantly, though it fluctuates with time. In the CO_2-doubling experiment (2xC), however, the conveyor keeps weakening long after the 70th year, when CO_2 stops increasing. Around 150th year, it stops weakening, and begin to intensify very slowly until it restores the original intensity by the 500th year. In the CO_2-quadrupling experiment (4xC), the conveyor keeps weakening beyond the 140th year, when CO_2 quadruples, and becomes very weak by the 200th year. The 4xC experiment was extended to 5,000th years by Stouffer and Manabe (2003). They found that conveyor remains weak until the 1,000th year, when it begins to re-intensify slowly. By the 1,700th year, the conveyor regains the original intensity.

The eventual re-intensification of the conveyor is attributable to the change in the distribution of water density, which results from the weakening of the conveyor during the first few hundred years of the two experiments (2xC and 4xC). As Fig. 9b shows, surface waters sink to depth around 60°N, but some of these waters rise slowly over very wide regions extending from 40°N to Southern Atlantic. As the upwelling of cold deep water weaken due to the weakening of conveyor, temperature of

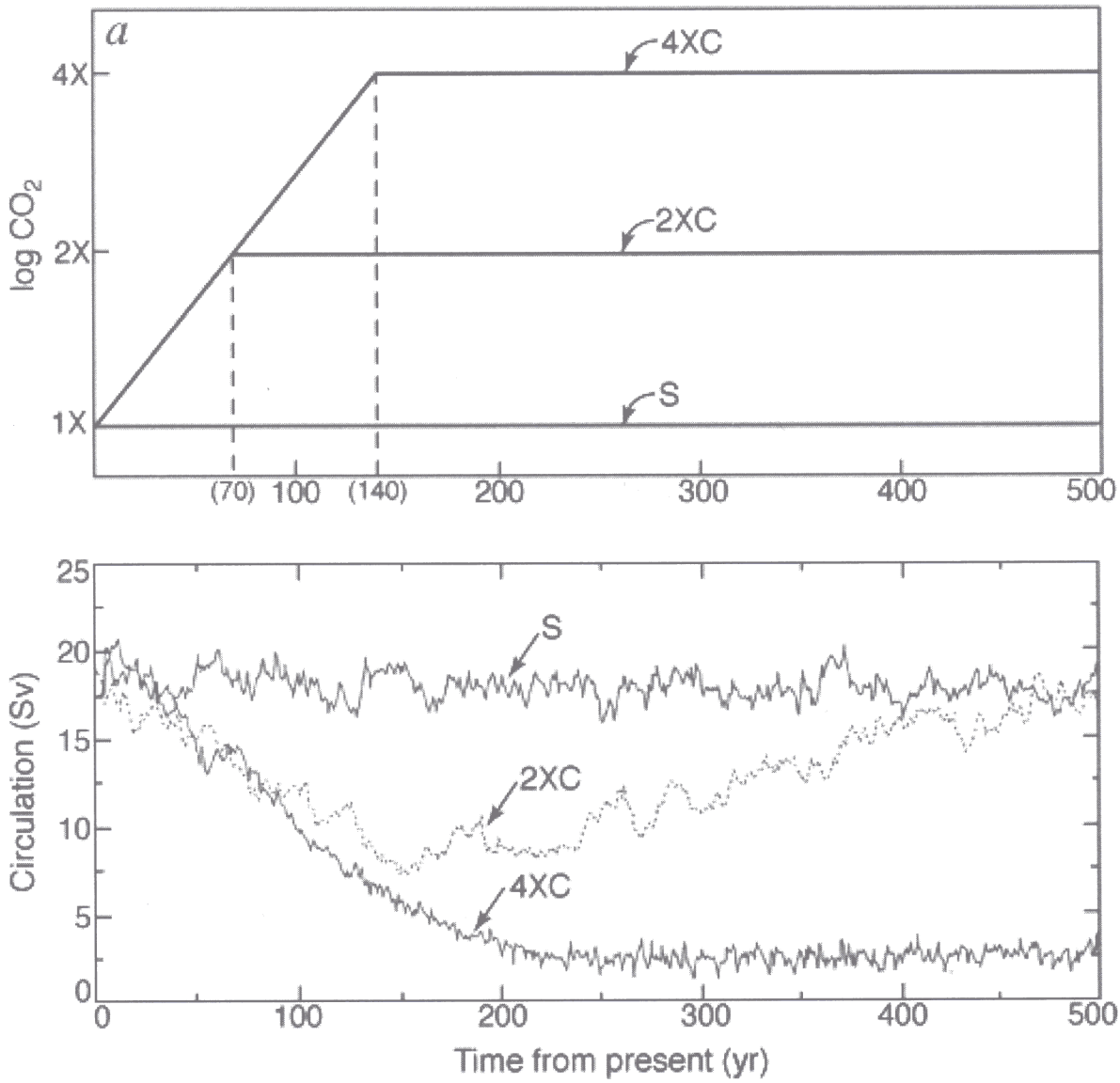

Fig. 10. Temporal variation of: a (top). logarithm of atmospheric CO_2 concentration: b (bottom). the intensity of the conveyor in the North Atlantic from the 4xC, 2xC, and S. Here the intensity is defined as the maximum value of the stream function that represents the meridional circulation in the North Atlantic.

the upper ocean layer increases in these regions. The resulting change in the distribution of water density appears to be responsible for the eventual recovery of the overturning circulation as discussed, for example, by Manabe and Stouffer (1993, 1994) and Stouffer and Manabe (2003). The timing of the reintensification of the conveyor is highly model-dependent (Cubasch et al. 2001). They are affected also by the rate of change in radiative forcing as shown by Stouffer and Manabe (1999).

2.6 Circumpolar Ocean

a. Time-dependent response

In the Circumpolar Ocean of the Southern Hemisphere, the Circumpolar Currents and deep overturning circulation prevails beneath

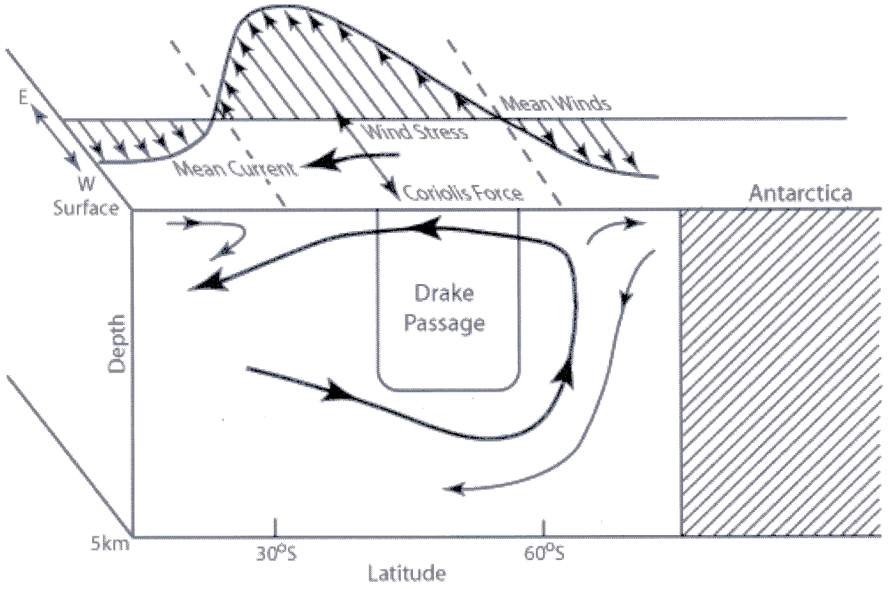

Fig. 11. A schematic of the prevailing surface winds in the Southern Hemisphere, and the overturning circulation, averaged around latitude circle, at the latitude of the Drake Passage. From Held (1993)

the strong westerly. Gill and Bryan (1971), Bryan et al. (1988), and Cox (1989) show that the deep overturning cell can not exist without the Drake Passage, which connects zonally the Circumpolar Ocean. As shown in Fig. 11 (Held 1993), zonal mean wind stress in the mixed layer must be balanced by the Coriolis force acting on an ageostrophic, northward current. On the other hand, the ageostrophic, southward return flow develops in the deep layer of ocean, where the Coriolis force acting on the return flow is compensated by the pressure difference across bottom relief. This is how the deep overturning cell develops in the Circumpolar Ocean, providing unusually strong coupling between the surface water and the deep ocean.

Figure 12 illustrates the streamfunction of the meridional overturning circulation obtained from the coupled model. In this figure, one can identify a deep overturning cell with upwelling around 60°S and sinking around 40°S. The presence of upwelling of relatively warm water on the southern half of the Current has been noted by Deacon (1937). As one can expect, the upwelling of deep water beneath cold surface water destabilizes the near-surface layer, inducing deep convection. This is why deep convective mixing predominates around 50–60°S, where the upwelling region is located.

Fig. 12. The streamfunction of the overturning circulation averaged zonally over all oceans of the coupled ocean-atmosphere model. Units are in Sverdrup, i.e., 10^6 m^3s^{-1}. From Manabe et al. (1991)

In the immediate vicinity of Antarctic Continent (e.g., Weddell and Ross Seas), where oceanic surface is cooled very intensely, deep

convection predominates due to the brine rejection, which results from freezing of sea water. The convective cooling of water in turn induces thermally driven, overturning circulation and is responsible for the deep vertical mixing of heat in the immediate vicinity of the Antarctic Continent (Fig. 12).

In addition to convection, so-called, isopycnal mixing (i.e., mixing along the surface of constant density) is also responsible for the downward heat transfer. Beneath the northern half of surface westerly winds (i.e., on the northern side of the Circumpolar front and associated Antarctic Circumpolar current), water converges at oceanic surface, and penetrates downward along the isopycnal surface, forming "intermediate water" with relatively low salinity.

Figure 13 illustrates the change in zonal mean temperature obtained from the coupled model. According to this figure, the penetration of positive temperature anomaly is relatively deep between 40°S and 65°S and in the immediate vicinity of the Antarctic Continent. Because of the vertical mixing of heat due to deep convection and isopycnal mixing, the effective thermal inertia is large in these regions, thereby delaying greatly the response of sea surface temperature in the Circumpolar Ocean of the Southern Hemisphere.

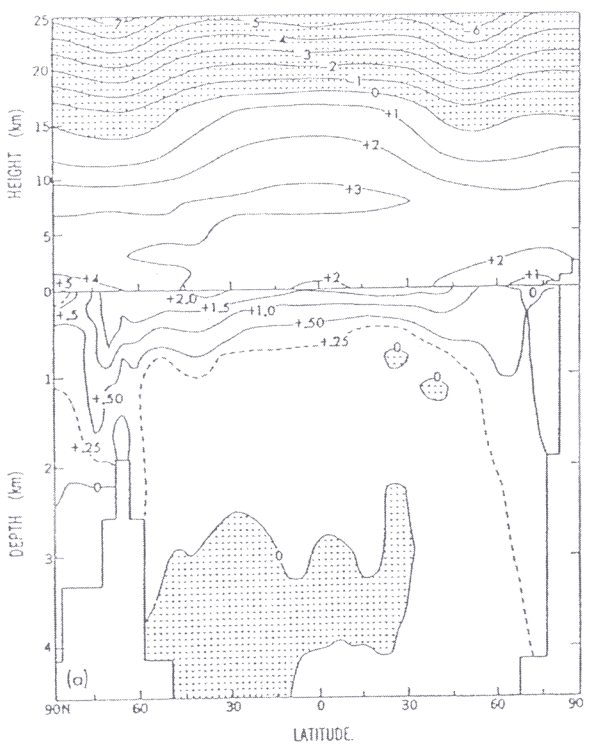

Fig. 13. Zonal mean temperature change (°C) of the coupled atmosphere-ocean model, which is realized by the ~70th year (i.e., the average from the 60th to 80th year) of the experiment, i.e., the time of the CO_2 doubling. From Manabe et al. (1991)

b. Mesoscale eddies

The most energetic oceanic motions occur with length scale of 10 to 100 km and is called mesoscale eddy. In the Circumpolar Ocean of the Southern Hemisphere, mesoscale eddies are very active, transferring heat across the Circumpolar Current. Thus, it is very desirable to incorporate the thermal and dynamical effect of mesoscale eddies into a coupled model. However, in view of the huge requirement of computer resources involved, it is not yet practical to use a coupled model with eddy-resolving oceans for the study of climate change. Clearly, there is a pressing need for the parameterization of mesoscale eddies.

Redi (1982) made an initial attempt to parameterize the isopycnal mixing of heat by mesoscale eddies. Cox (1989) simplified her parameterization and incorporated it into the oceanic component of the coupled model, which was used by Manabe et al. (1991) for the study presented here. As noted by Danabasoglu (1994), however, these eddies transport not only heat but also momentum, thereby inducing meridional overturning circulation. In the Circumpolar Ocean, the eddy-induced circulation flows in the opposite direction from the Deacon Cell. It is therefore likely that, in the Circumpolar Ocean, the intensities of upwelling and associated convective activity are overestimated in the Redi's parameterization, which does not include the effect of the induced circulation.

In order to eliminate the shortcoming of Redi's approach, Gent and McWilliams (1990) developed a parameterization, which includes not only the effect of the isopycnal mixing but also that of the eddy-induced overturning circulation. Incorporating the parameterization into an oceanic GCM, Danabasoglu et al. (1994) evaluated its impact upon the thermal and dynamical structure of the model ocean.

Since the publication of their study, the so-called G-M parameterization of mesoscale eddy has been incorporated in a majority of coupled models currently used for the projection of future climate change. As shown by Cubasch et al. (2001) in the last report of the Intergovermental Panel on Climate Change (2001), the projected changes of sea surface temperature obtained from these models is very small in the Circumpolar Ocean, in agreement with the result presented here.

One note, however, that the positive temperature anomaly of the Circumpolar Ocean does not penetrate as deeply in the model with the G-M parameterization (see Fig. 12 of Stouffer et al. 2006b, for example). It is essentially confined to the top 1.5 km layer of the ocean, indicating that much of the vertical mixing of heat is achieved through isopycnal mixing in the upper layer of the ocean. This is in contrast to the earlier result, which indicates the deep penetration of the warm anomaly in the Circumpolar Ocean (Fig. 13). In our opinion, the difference between the two results is attributable mainly to the parameterizations of mesoscale eddies. Because of the difference in the intensity of overturning circulation, the upwelling and associated convection is much weaker in the new result in the Circumpolar Ocean of the Southern Hemisphere. It is also noted that the oceanic convection found near the Antarctic coast is greatly reduced in the new result.

In the original G-M parameterization, it is assumed that the coefficient of the isopycnal mixing is constant everywhere. In the new model used by Stouffer et al. (2006), it varies geographically depending upon oceanic state. Unfortunately, its magnitude is highly uncertain. Therefore, we do not know how realistic is the intensity of the eddy-induced circulation obtained from the model. This is the main reason why it is premature to assume that the intensity of overturning circulation and associated convective activity in the Circumpolar Ocean is more realistic in the new than old model.

It is important to recall here that Dixon et al. (1996) successfully simulated the deep penetration of CFC-11 (i.e., tri-chloro-fluoro-methane) in the Circumpolar Ocean using the old model. Although the successful simulation is attributable in no small part to the compensation among the biases of the old model (low surface wind stress and excessive subgrid-scale mixing of heat), their study suggest that deep penetrative convection prevails in the Circumpolar Ocean as simulated by the old model.

The effect of meso-scale eddy may be investigated using an ocean model, which has high enough resolution to resolve meso-scale eddy (e.g., Henning and Vallis 2005). With the availability of increasingly powerful computers, it may soon become possible to use an eddy-resolving ocean model for the projection of global warming in the near future.

3. Observed changes

The radiative heat budget of the Earth is affected not only by the concentration of greenhouse gases but also the loading of aerosols that reflect and absorb incoming solar radiation (Penner et al. 2001). Using a coupled model developed at Hadley Center, Meteorological Office of the U.K., Mitchell et al. (1995) conducted global warming experiments with and without the thermal forcing of aerosols. They found that the model overestimates the warming during the 20 century, if it is forced by the observed increase in greenhouse gases alone. However, the model yields smaller and more realistic warming, if the thermal forcing includes the direct cooling effect of anthropogenic sulfate aerosols that have increased during the last several decades. Their study underscored the potential importance of aerosols such as sulfate, and has instigated many numerical experiments, in which coupled models are forced radiatively not only by greenhouse gases but also by various types of aerosols (Cubasch et al. 2001).

As demonstrated by Mitchell et al. (1995), one of the effective ways to evaluate the performance of a coupled model is to compare the simulated and observed change in surface temperature. With the availability of massive hydrographic data (Levitus et al. 1994), it has become feasible to compare the simulated and observed temperature change in the subsurface layers of ocean, leading to the pioneering studies by Levitus et al. (2000, 2001), and Barnett et al. (2001). Here, we describe some of the results they obtained.

The coupled ocean-atmosphere model used by

Levitus and his collaborators is similar to the model used by Manabe et al. (1991) except that it has twice as high a horizontal resolution as the earlier version. The model was forced by the observed changes in greenhouse gases, sulfate aerosols of the industrial and volcanic origins, and solar irradiance during the past century. Starting from three slightly different initial conditions, the numerical time integrations of the coupled model was repeated three times. In order to reduce the contamination from natural variability, the results from the three experiments are averaged. It was found that the global ocean heat content (calculated over the depth range of 0 to 3,000 m) increases by 19.7×10^{22} Joule over the period from 1955 to 1996. This is in agreement with the observed estimate (18.2×10^{22} Joule). However, there is a large amount of uncertainty associated with the observations because of the poor sampling of the global oceans, particularly the Southern Ocean. Averaged over the entire globe, the rate of heat uptake at the Earth's surface is 0.30 w/m^{-2} and 0.28 w/m^{-2} for the model and observations, respectively. These values are about 7% of 4 w/m^{-2}, i.e., the radiative forcing involved in the CO_2-doubling.

Barnett et al. (2001) performed similar numerical experiments using a coupled ocean-atmosphere model developed at the National Center for Atmospheric Research (NCAR), USA (Dai et al. 2001). In response to the anthropogenic forcing, the NCAR model yielded changes in heat content in most of the major oceans over the last forty five years that are highly similar to those observed. For example, the model successfully reproduces the deep penetration of positive temperature anomaly in the North Atlantic as compared with the North Pacific Ocean. Although the model indicates the deep penetration of positive temperature anomaly in the Circumpolar Ocean of the Southern Hemisphere, it was difficult to confirm it because of insufficient data coverage.

Figure 14 illustrates the geographical distribution of surface temperature anomaly for the year 2005 (Kenedy et al. 2006). It represents the difference in surface temperature between 2005 and the 30 year period centered around 1975. This figure shows that the warming is

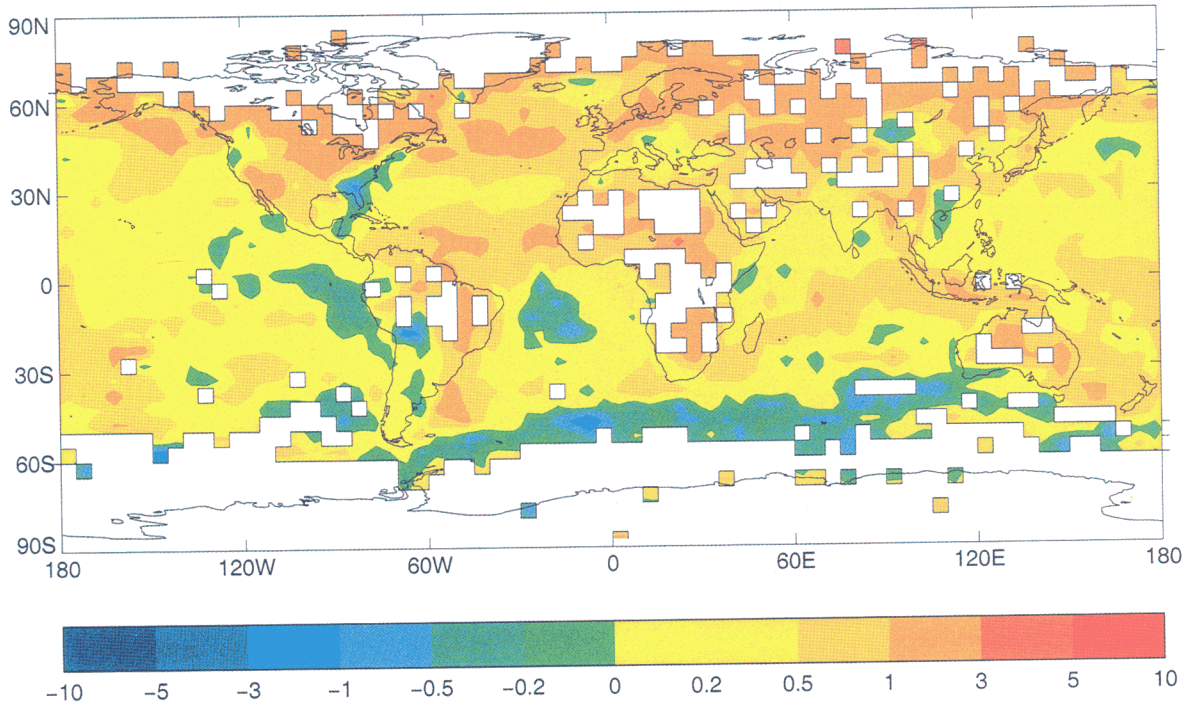

Fig. 14. Surface temperature anomalies (°C) (relative to 1961–90) for 2005 (Kenedy et al. 2006). The temperature value of each (5° latitude) × (5° longitude) pixel is derived from at least 1 month's data in each of four 3-month seasons (January to March etc). Data are from Brohan et al. (2006).

usually larger over continent than over ocean in qualitative agreement with the simulated change in surface air temperature shown in Fig. 3. In the Circumpolar Ocean of the Southern Hemisphere, one can identifies the areas of negative temperature anomaly in the Atlantic and Indian Ocean sector. On the other hand, positive anomaly extends to the southern end of data coverage. Zonally averaged over an entire latitude circle, the magnitude of anomaly is very small around 45–50°S, indicating that systematic warming is relatively small in the Circumpolar Ocean of Southern Hemisphere. Although the reliability of data is poor near the southern margin of data coverage, it is quite encouraging that the distribution of the observed 2005 anomaly of surface temperature appears to be consistent with the inter-hemispheric asymmetry in surface temperature change simulated by coupled models.

The recent report entitled "State of the Climate in 2005" (NOAA NODC, 2006) presents the time series of sea ice coverage over Arctic and Antarctic Oceans during the last 28 years, when satellite observation of sea ice is available. As noted by A.M. Whipple in the report, sea ice extent has been increasing since the late 1970's, though it is less than one percent per decade. On the other hand, it decreases by several percent per decade in the Arctic Ocean during the last quarter century. Obviously, it is desirable to have the sea ice record over much longer period of time. Nevertheless, the large inter-polar difference in the trend of sea ice coverage during the last several decades appears to be in qualitative agreement with the simulated changes in sea ice shown in Figs. 4 and 5, and is consistent with the inter-hemispheric asymmetry in sea surface temperature change discussed in this review.

The results from numerical experiments presented in Section 2.5 suggest that the Atlantic conveyor may begin to weaken as global warming proceeds. Based upon the analysis of five sets of transatlantic, hydrographic measurements taken during the last four decades, Bryden et al. (2005) suggested that the conveyor has slowed by about 30% between 1957 and 2004. However, more recent measurements they conducted indicate that the variation of conveyor within one year is as large as the change seen during the last few decades. It appears that continuous measurement over decades is needed for the detection of systematic change of the conveyor.

Based upon the analysis of the numerical experiments, in which CO_2-equivalent concentration of greenhouse gas is held fixed, Delworth et al. (1993) suggested that the intensity of the simulated conveyor fluctuates at multi-decadal time scales even in the absence of global warming. As discussed by Manabe et al. (2001), for example, there are various indirect evidences for the existence of the unforced fluctuation of the conveyor (e.g., Dansgaard et al. 1971; Delworth and Mann 2000). Thus, it may be premature to conclude that the weakening of the conveyor found by Bryden and his collaborators is attributable solely to global warming. Even-handed emphasis should be placed upon the monitoring and analysis of both forced and unforced variability of the conveyor in the future.

4. Concluding remarks

Using coupled ocean-atmosphere models, we have shown that oceans can plays a major role in delaying global warming and shaping its geographical distribution. It is very encouraging that many features of the observed changes in the climate system have begun to agree with those simulated by model as noted in the preceding section. However, it has been very difficult to confirm the apparent agreement, because the density and frequency of the observations are insufficient in many oceanic regions of the world, in particular, in the Circumpolar Ocean of the Southern Hemisphere. In order to validate the simulation of climate change by a coupled model, it is therefore essential to intensify our effort to monitor the whole World Ocean, not only at the surface but also in the subsurface layers.

Ocean and atmosphere exchange not only heat and water but also carbon dioxide. Currently, ocean is absorbing a substantial fraction of carbon dioxide that is released into the atmosphere due to industrial activity. In the global warming experiment described here, the coupled model is subjected to gradually increasing concentration of carbon dioxide, which is predetermined and is given as an input. In order predict the future change in CO_2 concentration of air and its effect on climate, however, it is necessary to construct a coupled model,

which explicitly treats the exchange of carbon dioxide among the atmosphere, ocean and continental surface. Such a model was recently constructed, for example, by Cox et al. (2000) and was used for the projection of future climate change. It is likely that an increasing emphasis is going to be placed on the study of the role of carbon cycle in future climate change.

References

Barnett, T.P., D.W. Pierce, and R. Schnur, 2001: Detection of anthropogenic climate change in the world's oceans. *Science*, **292**, 270–274.

Boyer, T.P., S. Levitus, J.I. Antonov, R.A. Localnini, and H.E. Garcia, 2005: Linear trends in salinity for the world ocean, 1955–1988. *Geophys. Res. Lett.*, **32**, L01604, doi: 10.1029/2004GL021791.

Broecker, W.S., 1991: The great ocean conveyor. *Oceanography*, **4**, 79–89.

Brohan, P., J.J. Kenedy, I. Harris, S.F.B. Tett, and P.D. Jones, 2006: Uncertainty estimates in regional and global observed temperature changes: a new data set from 1850. *J. Geophys. Res.*, in press.

Bryan, K., 1969: Climate and ocean circulation. III: The ocean model. *Mon. Wea. Rev.*, **97**, 806–827.

Bryan, K. and L.J. Lewis, 1979: A water mass model of world ocean. *J. Geophys. Res.*, **84(C5)**, 2503–2517.

Bryan, K., S. Manabe, and M.J. Spelman, 1988: Inter-hemispheric asymmetry in the transient response of a coupled ocean-atmosphere model to a CO_2 forcing. *J. Phys. Oceanogr.*, **18**, 851–867.

Bryan, K., F.G. Komro, S. Manabe, and M.J. Spellman, 1982: Transient climate response to increasing atmospheric carbon dioxide. *Science*, **215**, 56–58.

Bryden, H.L., H.R. Longworth, and S.A. Cunningham, 2005: Slowing of the Atlantic meridional overturning circulation at 25°N. *Nature*, **438**, 655–657.

Cox, M., 1989: An idealized model of the world oceans. Part 1: The global-scale water masses. *J. Phys. Oceanogr.*, **19**, 1730–1759.

Cox, P.M., R.A. Betts, C.D. Jones, S.A. Spall, and I.J. Totterdell, 2000: Acceleration of global warming due to carbon-cycle feedbacks in a coupled model. *Nature*, **408**, 184–187.

Cubasch, U. et al., 2001: Projection of future climate change. In *Climate Change 2001, The Science of Climate Change* Chapter 9 (eds Houghton, J.T. et al.) 527–582 (Cambridge University Press, Cambridge, 2001).

Dai, A., T.M.L. Wigley, B.A. Boville, J.T. Kiehl, and L.E. Buja, 2001: Climate of the twentieth and twenty-first centuries simulated by the NCAR climate system model. *J. Climate*, **14**, 485–519.

Danabasoglu, G., J.C. McWilliams, and P.R. Gent, 1994: The role of mesoscale tracer transports in the global circulation. *Science*, **264**, 1123–1126.

Dansgaard, W., J. Johnson, H.B. Clausen, and C.C. Langley Jr., 1971: Climate Record revealed by the Camp Century ice core. Pp 37–56 in late Cenozoic glacial ages. Edited by K.K. Trekian. Yale University Press, New Haven, Connecticut, USA.

Deacon, G.E.R., 1937: Note on the dynamics of southern ocean. *Discovery Report*, Cambridge University Press, **15**, 125–152.

Delworth, T.L. and M.E. Mann, 2000: Observed and simulated multidecadal variability in the North Atlantic. *Clim. Dyn.*, **16**, 671–676.

Delworth, T.L., S. Manabe, and R.J. Stouffer, 1993: Interdecadal variation of the thermohaline circulation in a coupled ocean-atmosphere model. *J. Climate*, **6**, 1993–2011.

Dixon, K.W., J.L. Bullister, R.H. Gamon, and R.J. Stouffer, 1996: Examining a coupled climate model using CFC-11 as an ocean tracer. *Geophys. Res. Lett.*, **26**, 2749–2752.

Dixon, K.W., T.L. Delworth, M.J. Spelman, and R.J. Stouffer, 1999: The influence of transient surface fluxes on North Atlantic overturning in a coupled GCM climate change experiment. *Geophys. Res. Lett.*, **26**, 2749–2752.

Gent, P.R. and J.C. McWilliams, 1990: Isopicnal mixing in ocean circulation models. *J. Phys. Oceanogr.*, **20**, 150–155.

Gill, A.E. and K. Bryan, 1971: Effect of geometry on the circulation of a three dimensional southern–hemisphere ocean model. *Deep-Sea Res.*, **18**, 685–721.

Gordon, A.L., 1986: Inter-ocean exchange of thermocline water and its influence on thermohaline circulation. *J. Geophys. Res.*, **91**, 5037–5046.

Gregory, J.M., K.M. Dixon, R.J. Stouffer, A.J. Weaver, E. Driesschaert, M. Eby, T. Fichefet, H. Hasumi, A. Hu, J.H. Jungclaus, I.V. Kamenkovich, A. Levermann, M. Montoya, S. Murakami, S. Nawrath, A. Oka, A.P. Sokolov, and R.B. Thorpe, 2005: A model intercomparison of changes in the Atlantic thermohaline circulation in response to increasing atmospheric CO_2 concentration. *Geophys. Res. Lett.*, **32**, L12703, doi:10.1029/2005GL023209.

Hansen, J., A. Lacis, D. Reind, G. Russel, P. Stone, I. Fung, R. Ruedy, and J. Lerner, 1984: Climate sensitivity: Analysis of feedback mechanisms. *Climate Process and Climate Sensitivity*, Maurice Ewing Series, J.E. Hansen and T. Takaha-

shi Eds., American Geophysical Union, 130–163.

Hansen, J., I. Fung, A. Lacis, D. Rind, S. Lebedeff, R. Ruedy, G. Russel, and P. Stone, 1988: Global climate change as forecast by the Goddard Institute for Space Studies three dimensional model. *J. Geophys. Res.*, **93**, 9341–9364.

Held, I.M., 1993: Large-scale dynamics and global warming. *Bull. Amer. Meteor. Soc.*, **74**, 228–241.

Henning, C.C. and G.K. Vallis, 2005: The effect of mesoscale eddies on the stratification and transport of an ocean with a circumpolar channel. *J. Phys. Oceanogr.*, **35**, 880–896.

Hoffert, M.I., A.J. Callegari, and C.T. Hsieh, 1980: The role of deep sea heat storage in the secular response to climatic forcing. *J. Geophys. Res.*, **85**, 6667–6679.

Kenedy, J., D. Pârker, and H. Coleman, 2006: Global and regional climate in 2005. *Weather*, **61**, 215–224.

Levitus, S., R.D. Gelfeld, T. Boyer, and D. Johonson, 1994: Rescue of the NODC and IOC data Archeology and Rescue Projects. Key to Oceanographic Records Documentation. No. 19 (National Oceanographic Data Center, Washington, DC).

Levitus, S., J.I. Antony, T.P. Boyer, and C. Stephens, 2000: Warming of the world ocean. *Science*, **287**, 2225–2229.

Levitus, S., J.I. Antonov, J. Wang, T.L. Delworth, K.W. Dixon, and A.J. Broccoli, 2001: Anthropogenic warming of Earth's climate system. *Science*, **292**, 267–270.

Manabe, S., 1969: Climate and ocean circulation: 1. The atmospheric circulation and hydrology of the Earth's surface. *Mon. Wea. Rev.*, **97**, 739–774.

Manabe, S. and K. Bryan, 1969: Climate calculation with a combined ocean-atmosphere model. *J. Atmos. Sci.*, **26(4)**, 786–789.

Manabe, S. and R.J. Stouffer, 1979: A CO_2 climate sensitivity study with a mathematical model of global climate. *Nature*, **282**, 491–493.

Manabe, S. and R.J. Stouffer, 1999: Are two modes of thermohaline circulation stable? *Tellus*, **51A**, 400–411.

Manabe, S. and R.J. Stouffer, 1993: Century-scale effects of increased atmospheric CO_2 on the ocean-atmosphere system. *Nature*, **364**, 215–218.

Manabe, S. and R.J. Stouffer, 1994: Multiple century response of a coupled ocean-atmosphere model to an increase in atmospheric carbon dioxide. *J. Climate*, **7**, 5–23.

Manabe, S., R.J. Stouffer, M.J. Spelman, and K. Bryan, 1991: Transient response of a coupled ocean atmosphere model to gradual changes of atmospheric CO_2. Part I: Annual mean response. *J. Climate*, **4**, 785–818.

Manabe, S., Spelman, M.J., and R.J. Stouffer, 1992: Transient response of a coupled ocean atmosphere model to gradual changes of atmospheric CO_2. Part II: Seasonal response. *J. Climate*, **5**, 105–126.

Manabe, S., T.R. Knutson, R.J. Stouffer, and T.L. Delworth, 2001: Exploring natural and anthropogenic variation of climate. *Quart. J. Roy. Meteor. Soc.*, **127**, 1–24.

Mitchell, J.F.B., T.C. Johns, J.M. Gregory, and F.B. Tett, 1995: Climate response to increasing levels of greenhouse gases and sulphate aerosols. *Nature*, **376**, 501–504.

NOAA NODC, 2006: State of climate in 2005. (eds K.A. Shein) 102pp. Special supplement to the *Bull. Amer. Meteor. Soc.*, **87 (6)**.

Penner, J.E. et al., 2001: Aerosols, their direct and indirect effect. In *Climate Change 2001, The Science of Climate Change* Chapter 5 (eds Houghton, J.T. et al.) 287–348, (Cambridge University Press, Cambridge, 2001).

Redi, M.H., 1982: Oceanic isopychnal mixing by coordinate rotation. *J. Phys. Oceanogr.*, **12**, 1154–1158.

Schneider, S.H. and C. Mass, 1975: Volcanic dust, sunspots and temperature trends. *Science*, **190**, 741–746.

Schneider, S.H. and S.L. Thompson, 1981: Atmospheric CO_2 and climate: Importance of transient response. *J. Geophys. Res.*, **86(C4)**, 3135–3147.

Stouffer, R.J. and S. Manabe, 1999: Response of a coupled ocean-atmosphere model to increasing atmospheric carbon dioxide: Sensitivity to the rate of increase. *J. Climate-Part I*, **12**, 2224–2237.

Stouffer, R.J. and S. Manabe, 2003: Equilibrium response of thermohaline circulation to a large changes in atmospheric CO_2 concentration. *Clim. Dyn.*, **20**, 759–773.

Stouffer, R.J., S. Manabe, and K. Bryan, 1989: Interhemispheric asymmetry in climate response to a gradual increase of atmospheric CO_2. *Nature*, **342**, 660–662.

Stouffer, R.J., et al., 2006a: Investigating the cause of the response of the thermohaline circulation to past and future climate change. *J. Climate*, **19**, 1365–1387.

Stouffer, R.J., et al., 2006b: GFDL's CM2 global coupled climate models. Part IV: Idealized Climate Response. *J. Climate*, **19**, 723–740.

Washington, W.M. and G.A. Meehl, 1989: Climate sensitivity due to increased CO_2: Experiment with a coupled atmosphere and ocean general circulation model. *Clim. Dyn.*, **4**, 1–38.